SP Science Press

ARTICLE

Effect of V Content on Microstructure, Phase Transformation Behavior and Microhardness of Equiatomic NiTi Shape Memory Alloy

Gan Chunlei[1,3], Chen Zhiwei[1,2,3], Li Xiaohui[1,3], Zhou Nan[1,3], Qian Jianqing[2], Zheng Kaihong[1,3], Li Jilin[1,3]

[1] Institute of New Materials, Guangdong Academy of Sciences, Guangzhou 510650, China; [2] College of Metallurgical Engineering, Anhui University of Technology, Maanshan 243002, China; [3] Guangdong Provincial Key Laboratory of Metal Toughening Technology and Application, Guangzhou 510650, China

Abstract: The effect of vanadium (V) content on the microstructure, phase transformation behavior, and microhardness of the as-cast equiatomic NiTi shape memory alloy was investigated by optical microscope (OM), scanning electron microscope (SEM) equipped with an energy dispersive spectrometer (EDS), X-ray diffraction (XRD), differential scanning calorimetry (DSC) and Vickers microhardness tester. Results indicate that the as-cast $Ni_{50-x/2}Ti_{50-x/2}V_x$ alloys with equiaxed grains consist mainly of B19' and Ti_2Ni phases when V content is 0.5at%, above which $Ni_{50-x/2}Ti_{50-x/2}V_x$ (x=1.5~3.5, at%) alloys exhibit a three-phase structure consisting of B19', Ti_2Ni and V-rich phases, and the V-rich phases are more segregated at grain boundaries with the increase of V content. Further analysis reveals that both $Ni_{49.75}Ti_{49.75}V_{0.5}$ and $Ni_{49.25}Ti_{49.25}V_{1.5}$ alloys show a one-stage B2↔B19' transformation. However, a two-stage B2↔R↔B19' transformation occurs in $Ni_{48.75}Ti_{48.75}V_{2.5}$ and $Ni_{48.25}Ti_{48.25}V_{3.5}$ alloys although R-phase transformation partially overlaps B19' martensitic transformation upon cooling. The transformation temperatures drop down with increasing the V content, which is attributed to the increase of Ni/Ti ratio in the matrix. In addition, as V element increases from 0.5at% to 3.5at%, the microhardness of the alloys first decreases and then remains almost unchanged.

Key words: V content; NiTi shape memory alloys (SMAs); microstructure; martensite transformation; microhardness

Equiatomic NiTi alloy is one of the most important shape memory alloys (SMAs) because it exhibits excellent functional properties such as unique shape memory effect, pseudoelasticity, corrosion resistance and good biocompatibility[1-4]. The superior properties of NiTi SMAs are considered to be ascribed to martensitic transformation which can be thermally-induced or stress-induced[5-7]. Moreover, the alloy composition is now recognized as another important factor that has an essential effect on phase transformation behavior of NiTi SMAs[8]. The addition of the third element in NiTi matrix strongly affects the martensite transformation temperature, transformation behavior and service life. Therefore, over the past decades, considerable effort has been invested to modify the chemical properties of NiTi-based

SMAs[9,10].

In recent years, it has been reported that adding vanadium (V) into NiTi alloys can obtain higher absorbed energy[11], induce the B2 ↔ B19 transformation[12] and decrease the transformation temperature[13]. Unfortunately, so far, systematic investigation on the effect of V content on the structure, transformation behavior and mechanical properties of NiTi SMAs is not yet sufficient. More work is needed to further clarify the significant influence of V addition. In the present work, the non-consumable vacuum arc melting technique was employed to prepare a set of alloys with nominal compositions (at%) of $Ni_{50-x/2}Ti_{50-x/2}V_x$, where x is equal to 0.5, 1.5, 2.5 and 3.5. The effect of V content on the microstructure, phase transformation behavior, and mechanical properties of

NiTi SMAs was elucidated.

1 Experiment

1.1 Sample preparation

In the present study, the non-consumable vacuum arc melting technique was used to prepare a series of alloys with the following compositions (at%): $Ni_{50-x/2}Ti_{50-x/2}V_x$ alloy with x=0.5, 1.5, 2.5, 3.5, namely, $Ni_{49.75}Ti_{49.75}V_{0.5}$, $Ni_{49.25}Ti_{49.25}V_{1.5}$, $Ni_{48.75}Ti_{48.75}V_{2.5}$, and $Ni_{48.25}Ti_{48.25}V_{3.5}$ alloys (nominal compositions), respectively. Prior to melting, the bell furnace was evacuated three times to the pressure of $4×10^{-3}$ Pa and filled back with argon (purity 99.9vol%). Small NiTi ingots (about 20 g) with nickel (purity 99.99wt%), titanium (purity 99.99wt%), and vanadium (purity 99.99wt%) were melted and remelted at least five times in a water-cooled copper crucible (water temperature: 18 °C). In order to remove residual oxygen, a pure titanium button as a getter was also melted. The button sample was turned over after each arc melting step, and this procedure was repeated to promote thorough mixing. Fig. 1 shows morphologies and sizes of the as-cast button samples of NiTiV SMAs produced by non-consumable vacuum arc melting technique.

1.2 Microstructure observation and phase analysis

A solution of 10vol% HF, 40vol% HNO_3 and 50vol% distilled water was used to grind, polish and etch for 10 s to prepare samples for optical and electronic microscopy analysis. The microstructures were observed by both a DMI3000M Leica optical microscope (OM) and a JEOL JXA-8100 scanning electron microscope (SEM) equipped with an energy dispersive spectrometer (EDS). The EDS analysis was also performed to characterize various precipitates. The X-ray diffraction (XRD) was employed at the ambient temperature using a Bruker D8 Advance XRD with filtered Cu Kα radiation to determine different phases. In order to eliminate the effect of heterogeneity in the button samples resulting from different cooling rates, all samples were taken from the same position.

1.3 Transformation behavior analysis

The thermally-induced phase transformation behavior was analyzed by a differential scanning calorimeter (DSC) thermal analyzer from -150 °C to 100 °C with a heating and cooling rate of 5 °C·min^{-1}. The following single cycle was carried out: (1) heating to 100 °C and holding for 5 min; (2) recording the data of a full transformation cycle of cooling to -150 °C and

Fig.1 Morphologies and sizes of as-cast $Ni_{50-x/2}Ti_{50-x/2}V_x$ SMAs: (a) $Ni_{49.75}Ti_{49.75}V_{0.5}$, (b) $Ni_{49.25}Ti_{49.25}V_{1.5}$, (c) $Ni_{48.75}Ti_{48.75}V_{2.5}$, and (d) $Ni_{48.25}Ti_{48.25}V_{3.5}$

holding for 5 min; (3) heating back to 100 °C. During DSC testing, a slow continuous Ar flow was pumped through the entire DSC chamber to minimize oxidation of Ti; thus the best homogeneity of temperature was achieved and moisture was removed. The transformation temperatures were obtained by "Pyris Data Analysis" software.

1.4 Mechanical characterization

Samples for microhardness measurements were first mechanically ground and polished to smooth surface. Then the samples were measured at room temperature by an EM-1500L Vickers microhardness tester under a load of 500 g for duration of 15 s, and two adjacent test points were 0.3 mm apart. For each sample, the average microhardness value was recorded from at least ten test readings.

2 Results and Discussion

2.1 Effect of V content on the microstructure

Fig. 2 shows the evolution of the typical microstructures of $Ni_{50-x/2}Ti_{50-x/2}V_x$ SMAs with increasing the V content. It can be seen that the microstructure with the equiaxed grains is homogenous, and there are almost no evident differences among the four samples of $Ni_{49.75}Ti_{49.75}V_{0.5}$, $Ni_{49.25}Ti_{49.25}V_{1.5}$, $Ni_{48.75}Ti_{48.75}V_{2.5}$, and $Ni_{48.25}Ti_{48.25}V_{3.5}$ SMAs in terms of morphologies. However, there is a slight difference in grain size as a whole with the increase of V content, and a smaller grain size seems to be obtained as the V atomic ratio in the alloy increases to 3.5at%. Therefore, it can be concluded that the V element has relatively small influence on the grain size of equiatomic NiTi SMAs which were all processed under identical conditions. In addition, it is apparent from Fig.2 that there is a homogeneous distribution of dark precipitates in the four alloys.

Table 1 displays the chemical compositions of the matrix in $Ni_{50-x/2}Ti_{50-x/2}V_x$ SMAs shown in Fig.2, which are determined by EDS. The element V of $Ni_{49.75}Ti_{49.75}V_{0.5}$ alloy is too low to analyze its level. It can be found that the amount of V atoms in the solid solution of the NiTi matrix increases with increasing the V content. Further analysis shows that there is a large reduction in the V content between the nominal and measured compositions in the NiTi matrix. It indicates that all matrices in Fig.2 are NiTi SMAs containing part of V atoms in solid solution, which can improve the strength of $Ni_{50-x/2}Ti_{50-x/2}V_x$ SMAs due to the solid-solution strengthening effect.

Further analysis shows that another part of V atoms may exist in the form of precipitates. In order to confirm this, an area-scanning mode was used to determine the distribution state of V element in NiTi-SMAs by the EDS technique, and representative locations are given in Fig.3. It can be deduced that precipitates in dark color are V-rich phases along grain boundaries. The larger the adding amount of V element, the more the V-rich phases at grain boundaries. This strongly implies that the V-rich phase tends to enrich at grain boundaries with increasing the V content. Meanwhile, this also means that more V atoms exist at grain boundaries and less V atoms reamin in the matrix.
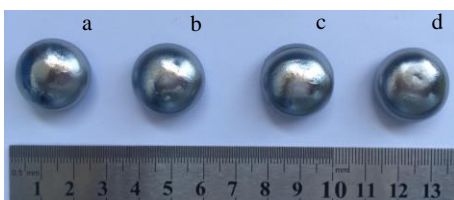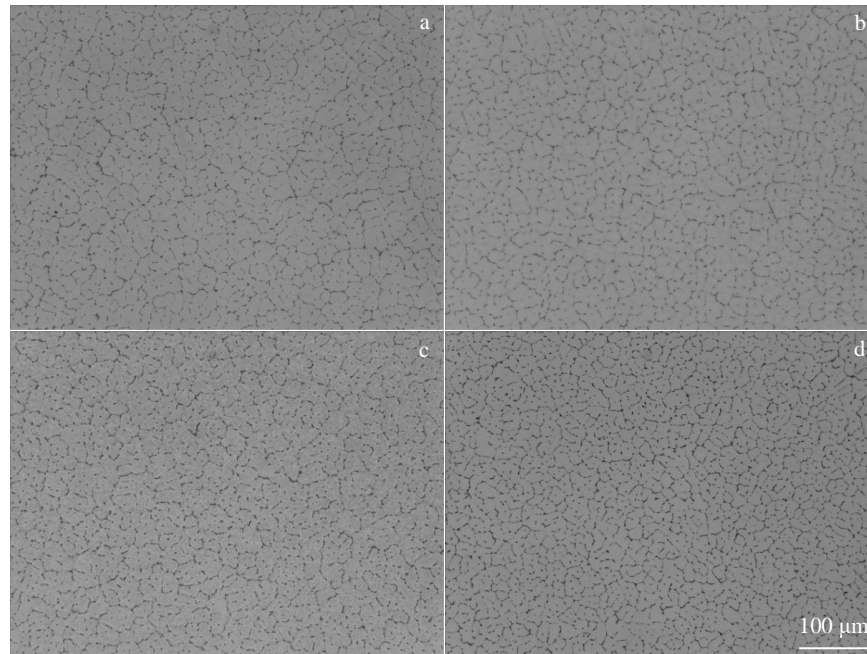
Fig.2 OM microstructures of $Ni_{49.75}Ti_{49.75}V_{0.5}$ (a), $Ni_{49.25}Ti_{49.25}V_{1.5}$ (b), $Ni_{48.75}Ti_{48.75}V_{2.5}$ (c), and $Ni_{48.25}Ti_{48.25}V_{3.5}$ (d) alloys

Table 1 EDS measured compositions of the matrix in as-cast $Ni_{50-x/2}Ti_{50-x/2}V_x$ alloys

Sample	Element content/at%				Ni/Ti
	Ni	Ti	V	Total	
$Ni_{49.75}Ti_{49.75}V_{0.5}$	49.06	50.94	-	100	0.963
$Ni_{49.25}Ti_{49.25}V_{1.5}$	48.77	50.24	0.99	100	0.971
$Ni_{48.75}Ti_{48.75}V_{2.5}$	48.84	49.54	1.62	100	0.986
$Ni_{48.25}Ti_{48.25}V_{3.5}$	48.57	48.74	2.68	100	0.997

2.2 Effect of V content on the phase formation

Fig.4 shows the XRD patterns of $Ni_{50-x/2}Ti_{50-x/2}V_x$ SMAs with different V contents at room temperature. XRD pattern of the $Ni_{49.75}Ti_{49.75}V_{0.5}$ alloy shows that typical monoclinic B19' martensite and Ti_2Ni phases are identified and no other phases are found. Other three XRD patterns are similar to each other, and B19' and $NiTi_2$ as the main phases are detected for all these four samples. XRD results also show that the V phase can only be detected in the sample with V contents above 0.5at% . Moreover, the diffraction intensity of the V phase increases evidently with increasing the V content, suggesting that more V addition can promote the formation of the V phase. According to XRD patterns and EDS analysis, the V-rich phase at grain boundaries contains substantial amounts of
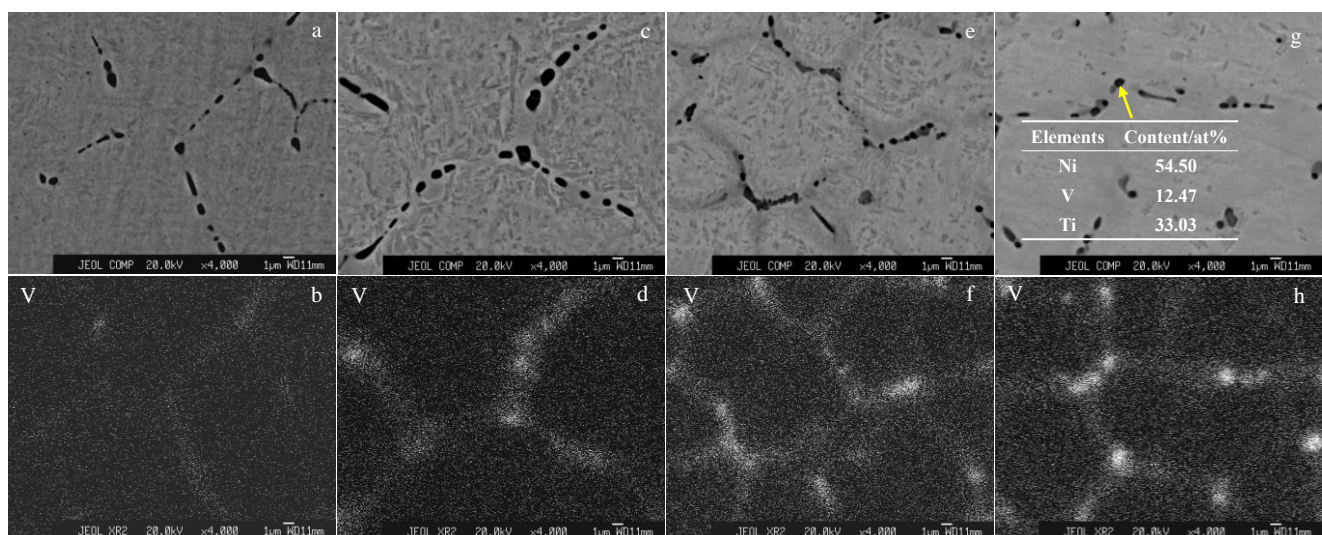

Elements	Content/at%
Ni	54.50
V	12.47
Ti	33.03

Fig.3 EDS results of distribution of V element in as-cast $Ni_{49.75}Ti_{49.75}V_{0.5}$ alloy (a, b), $Ni_{49.25}Ti_{49.25}V_{1.5}$ alloy (c, d), $Ni_{48.75}Ti_{48.75}V_{2.5}$ alloy (e, f) and $Ni_{48.25}Ti_{48.25}V_{3.5}$ alloy (g, h)
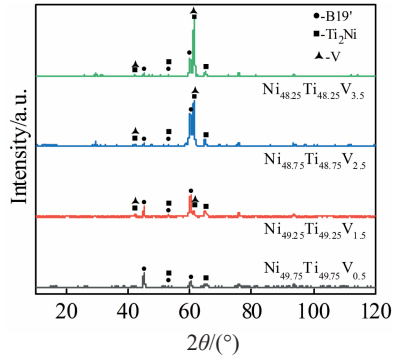
Fig.4　XRD patterns of $Ni_{49.75}Ti_{49.75}V_{0.5}$, $Ni_{49.25}Ti_{49.25}V_{1.5}$, $Ni_{48.75}Ti_{48.75}V_{2.5}$, and $Ni_{48.25}Ti_{48.25}V_{3.5}$ alloys

Ni and Ti. According to the PDF standard card, the V phase which exhibits a bcc structure with a lattice parameter of 0.303 nm is supposed to be $V_9(Ni,Ti)$, which is in agreement with Ref. [14]. It is indicated that lots of V atoms are consumed in forming the $V_9(Ni,Ti)$ phase at grain boundaries, which also helps explain why the content of V atoms in the NiTi matrix is less than the nominal composition.

Further analysis manifests that there are Ti_2Ni phases in as-cast $Ni_{50-x/2}Ti_{50-x/2}V_x$ alloys when V element is added to NiTi SMAs. The reason for the formation of Ti_2Ni phases may be deduced as follows. It is evident in Table 1 and Fig.3 that the V-rich phase contains substantial amounts of Ni and Ti and that the Ni/Ti ratio is less than 1. It is well known that Ti_2Ni phases tend to exist in the Ti-rich NiTi binary alloys[15]. This implies that the formation of the V-rich phase can result in a significant depletion of Ni in the matrix. In consequence, the matrix becomes relatively excessive in Ti, which leads to the formation of the Ti_2Ni phase. It can be easily understood according to the Ni-Ti binary phase diagram[16]. This result is well verified by the XRD results in Fig.4.

2.3 Effect of V content on transformation behavior

In order to investigate martensitic transformation behavior of the as-cast $Ni_{50-x/2}Ti_{50-x/2}V_x$ SMAs, DSC measurements were carried out and then typical DSC curves are depicted in Fig.5. It can be seen from Fig.5a and 5b that only exothermic and endothermic peaks are observed in the DSC curves of $Ni_{50-x/2}Ti_{50-x/2}V_x$ SMAs with lower V contents for $x=0.5$ and $x=1.5$ on each cooling and heating curve, respectively. The DSC peaks in these curves are ascribed to the $B2 \leftrightarrow B19'$ transformation. In contrast to the curves of Fig.5a and 5b, two exothermic and endothermic peaks in the heating and cooling processes of $Ni_{48.75}Ti_{48.75}V_{2.5}$ and $Ni_{48.25}Ti_{48.25}V_{3.5}$ alloys are found on each cooling and hearing curve, respectively. DSC peaks in Fig.5c and 5d are believed to result from the two-stage $B2 \leftrightarrow R \leftrightarrow B19'$ transformation. In consequence, it can be concluded that transformation behavior of the as-cast $Ni_{50-x/2}Ti_{50-x/2}V_x$ SMAs changes from the one-stage $B2 \leftrightarrow B19'$ to two-stage $B2 \leftrightarrow R \leftrightarrow B19'$ by increasing the V content.

From Fig.5, it can be found that transformation behavior of the as-cast $Ni_{50-x/2}Ti_{50-x/2}V_x$ alloys depends largely on V content. The $B2 \leftrightarrow B19'$ transformation occurs when V content increases to 1.5at%, above which the $B2 \leftrightarrow R \leftrightarrow B19'$ transformation occurs. This means that the involvement of R phase occurs under certain conditions prior to transformation to B19', although the $B2 \rightarrow R$ transformation is not separated clearly from the $R \rightarrow B19'$ transformation during cooling. This feature is believed to be related to the amount of solute atoms[17-19]. It can be found from Fig. 2 that the grain size decreases
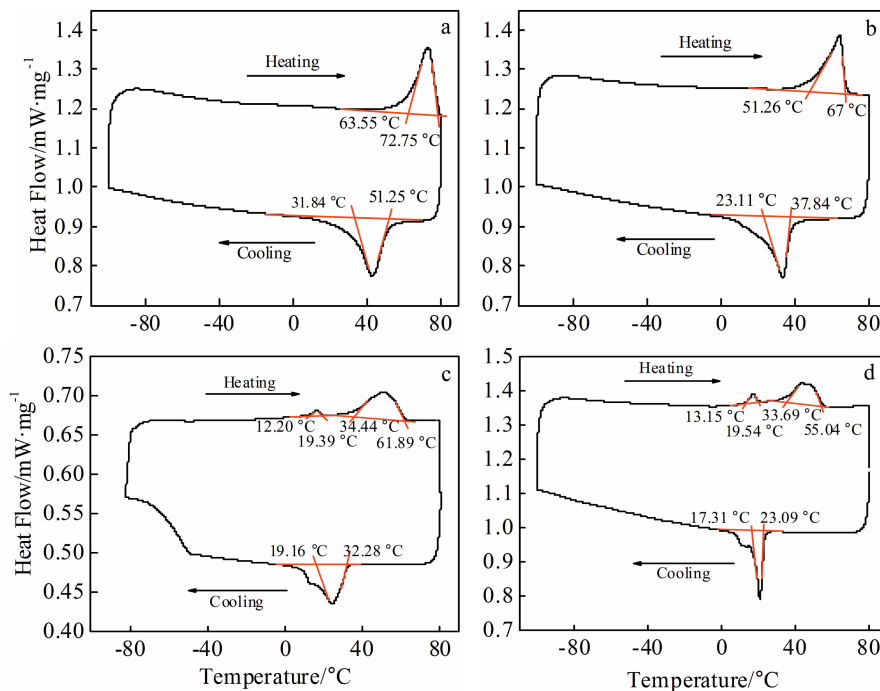

Fig.5　DSC curves for $Ni_{49.75}Ti_{49.75}V_{0.5}$ (a), $Ni_{49.25}Ti_{49.25}V_{1.5}$ (b), $Ni_{48.75}Ti_{48.75}V_{2.5}$ (c), and $Ni_{48.25}Ti_{48.25}V_{3.5}$ (d) alloys

gradually with increasing the V content, leading to the increase of interface energy. As a result, the resistance to martensitic transformation increases. In the meanwhile, the solubility of V in NiTi matrix increases continuously and the solid solution strengthening effect is also enhanced. The stability of the matrix increases. Therefore, the temperature of martensitic transformation decreases gradually. However, the temperature of phase transition decreases less since V element has relatively small effect on phase transformation properties of NiTi alloy with increasing the V content. When V content is 2.5at% and 3.5at%, V phases which have the same crystal structure and similar lattice constants as B2 austenite matrix form. Consequently, the reverse martensite transformation, namely austenite transformation, is inhibited. Therefore, during the heating process, martensite preferentially forms R phase and the second-order phase transition of B19'→R→B2 occurs.

As further examining the DSC curves in Fig.5a~5d, it can be found that the transformation temperatures for the austenitic and martensitic transformations decrease distinctly with increasing the V content. The martensitic transformation temperature (M_s, M_f) and the reverse phase transformation temperatures (A_s, A_f) of the experimental alloys are summarized in Table 2. This feature is attributed to the variation of Ni/Ti ratio in the NiTi matrix. V content and ratio of Ni to Ti are determined from compositions of matrices measured from EDS. It is well known that martensitic phase transformation temperature is significantly dependent on the Ni content in the NiTi matrix[20-22]. And in general, an increase of 1at% in Ni content in the matrix will give rise to the decrease of martensitic transformation temperature up to more than 100 °C [23]. This is consistent with the expected increase in the Ni content of the matrix. As discussed above, the addition of V not only leads to the formation of the V-rich phase, but also gives rise to an increase of the Ni/Ti ratio of the matrix. Therefore, the Ni/Ti ratio in the matrix increases with increasing the V content, resulting in a decrease in the martensitic transformation temperature.

2.4 Effect of V content on microhardness

Fig. 6 illustrates the Vickers microhardness of the as-cast $Ni_{49.75}Ti_{49.75}V_{0.5}$, $Ni_{49.25}Ti_{49.25}V_{1.5}$, $Ni_{48.75}Ti_{48.75}V_{2.5}$, and $Ni_{48.25}Ti_{48.25}V_{3.5}$ alloys, the average microhardness values of which are 2210, 2020, 2050, and 2000 MPa, respectively. The microhardness decreases with increasing the V content, and there is a large reduction from $Ni_{49.75}Ti_{49.75}V_{0.5}$ to $Ni_{49.25}Ti_{49.25}V_{1.5}$ alloys. However, the microhardness remains almost
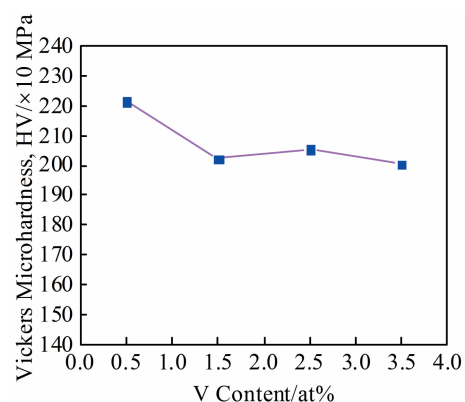
Fig. 6   Vickers microhardness as a function of V content for $Ni_{50-x/2}Ti_{50-x/2}V_x$ SMAs

unchanged as the V content continues to increase. According to the XRD and SEM analyses, this phenomenon may be caused by the effect of the solid-solution strengthening and the increase in the volume fraction of the bcc phase upon addition of V element. Firstly, as the Ti_2Ni phase is hard, the $Ni_{49.75}Ti_{49.75}V_{0.5}$ alloy is significantly stronger when the V content is lower, for example, 0.5at%. Secondly, the bcc phase is soft since it has multiple slip systems resulting in relatively low slip resistance. This means that alloys with more bcc phases will get softer. The primary factor for the large decrease in microhardness from the $Ni_{49.75}Ti_{49.75}V_{0.5}$ to the $Ni_{49.25}Ti_{49.25}V_{1.5}$ alloy is the substantial increase of the volume fraction of the V phase. As the V content is further increased, the microhardness from $Ni_{49.25}Ti_{49.25}V_{1.5}$ to $Ni_{48.25}Ti_{48.25}V_{3.5}$ alloy is in almost constant level. This can be ascribed to the fact that a balance between strengthening effects such as the solid-solution strengthening of V atom and the formation of much more bcc phase is achieved. As a result, the microhardness remains almost unchanged.

3 Conclusions

1) The microstructures of the as-cast $Ni_{50-x/2}Ti_{50-x/2}V_x$ SMAs consisting of equiaxed grains are very homogeneous and V-rich phases are more segregated at grain boundaries with the increase of V content.

2) The as-cast $Ni_{50-x/2}Ti_{50-x/2}V_x$ alloy mainly consists of B19' phase and Ti_2Ni phase when V content is 0.5at%, above which $Ni_{50-x/2}Ti_{50-x/2}V_x$ alloys exhibit a three-phase structure consisting of B19' phase, Ti_2Ni phase and V-rich phase.

3) The B2 ↔ B19' transformation occurs in $Ni_{49.75}Ti_{49.75}V_{0.5}$ and $Ni_{49.25}Ti_{49.25}V_{1.5}$ alloys. However, the B2 ↔ R ↔ B19' transformation occurs in $Ni_{48.75}Ti_{48.75}V_{2.5}$, and $Ni_{48.25}Ti_{48.25}V_{3.5}$ alloys although R-phase transformation partially overlaps B19' martensitic transformation upon cooling. The transformation temperatures decrease largely with increasing the V content due to the increase of Ni/Ti ratio in the matrix.

4) When the V content is 0.5at%, the microhardness of the $Ni_{49.75}Ti_{49.75}V_{0.5}$ alloy is 2210 MPa. With further increasing the V content, the microhardness of $Ni_{49.25}Ti_{49.25}V_{1.5}$ and

Table 2   Phase transformation temperature of as-cast $Ni_{50-x/2}Ti_{50-x/2}V_x$ SMAs (°C)

x	A_s	A_f	R_s	R_f	M_s	M_f
0.5	63.55	72.75	-	-	51.25	31.84
1.5	51.26	67.00	-	-	37.84	23.11
2.5	34.44	61.89	12.20	19.39	32.38	19.16
3.5	33.69	55.04	13.15	19.54	23.09	17.31

$Ni_{48.25}Ti_{48.25}V_{3.5}$ alloys remains almost unchanged.

References

1　Kaya I, Tobe H, Karaca H E *et al. Materials Science Engineering A*[J], 2016, 678: 93

2　Jaureguizahar S M, Chapetti M D, Yawny A. *International Journal of Fatigue*[J], 2018, 16: 300

3　Marattukalam J J, Balla V K, Das M *et al. Journal of Alloys and Compounds*[J], 2018, 744: 337

4　Toker S M, Canadinc D. *Materials Science Engineering C*[J], 2014, 40: 142

5　Elibol C, Wagner M F X. *Materials Science Engineering A*[J], 2015, 621: 76

6　Sun B, Fu M W, Lin J P *et al. Materials Design*[J], 2017, 131: 49

7　Chen Z B, Qin S J, Shang J X *et al. Intermetallics*[J], 2018, 94: 47

8　Velmurugan C, Senthilkumar V, Dinesh S *et al. Materials Today: Proceedings*[J], 2018, 5: 14 597

9　Frenzel J, Wieczorek A, Opahle I *et al. Acta Materialia*[J], 2015, 90: 213

10　Yuan Zhishan, Lin Dezhi, Cui Yue *et al. Rare Metal Materials and Engineering* [J], 2018, 47(7): 2269 (in Chinese)

11　Mao H, Yang H, Shi X *et al. Materials Letters*[J], 2018, 228: 391

12　Jang J Y, Chun S J, Choi E *et al. Materials Research Bulletin*[J], 2012, 47: 2939

13　Lin H, Lin K, Chang S *et al. Journal of Alloys and Compounds* [J], 1999, 284: 213

14　Lin H C, Yang C H, Lin M C *et al. Journal of Alloys and Compounds*[J], 2008, 499: 119

15　Nam T H, Lee J H, Jung D W *et al. Materials Science Engineering A*[J], 2007, 449-451: 1041

16　Qin Q H, Peng H B, Fan Q C. *Journal of Alloys and Compounds* [J], 2018, 739: 873

17　Kim J H, Jung K T, Noh J P *et al. Journal of Alloys and Compounds*[J], 2013, 577: 200

18　Chun S J, Noh J P, Yeom J T *et al. Intermetallics*[J], 2014, 46: 91

19　Hsieh S F, Wu S K, Lin H C *et al. Journal of Alloys and Compounds*[J], 2005, 387: 121

20　Otsuka K, Ren X. *Progress in Materials Science*[J], 2005, 50: 511

21　Liu A L, Cai W, Gao Z Y *et al. Materials. Science Engineering A* [J], 2006, 438-440: 634

22　Liu A L, Gao Z Y, Gao L. *Journal of Alloys and Compounds*[J], 2007, 437: 339

23　Frenzel J, George E P, Dlouhy A *et al. Acta Materialia*[J], 2010, 58(9): 3444

V 含量对等原子比 NiTi 形状记忆合金微观组织、相变行为和显微硬度的影响

甘春雷[1,3]，陈志伟[1,2,3]，黎小辉[1,3]，周　楠[1,3]，钱健清[2]，郑开宏[1,3]，李继林[1,3]

(1. 广东省科学院新材料研究所，广东 广州 510650)

(2. 安徽工业大学 冶金工程学院，安徽 马鞍山 243002)

(3. 广东省金属强韧化技术与应用重点实验室，广东 广州 510650)

摘　要：采用光学显微镜、扫描电子显微镜、X射线衍射仪、差示扫描量热仪和显微硬度计等测试手段，研究了V含量对等原子比NiTi形状记忆合金微观组织、相变行为和显微硬度的影响规律。结果表明：当V含量为0.5at%时，具有等轴晶组织的NiTiV形状记忆合金包含B19'和Ti_2Ni相；当V含量大于0.5at%时，NiTiV形状记忆合金形成B19'相、Ti_2Ni相和V的富集相，并且随着V含量增加，V的富集相越来越多聚集于晶界。进一步分析表明，$Ni_{49.75}Ti_{49.75}V_{0.5}$ 和 $Ni_{49.25}Ti_{49.25}V_{1.5}$ 形状记忆合金发生了 B2↔B19'的一级相变，而 $Ni_{48.75}Ti_{48.75}V_{2.5}$ 和 $Ni_{48.25}Ti_{48.25}V_{3.5}$ 形状记忆合金发生了 B2↔R↔B19'的二级相变，尽管降温过程中同时发生了部分的R相变与B19'马氏体相变。随着V含量增加，相变温度随着V含量增加逐渐降低，其主要原因是Ni/Ti比例的增加。此外，随着V含量增加，合金的显微硬度值呈现先降低然后几乎保持不变的变化规律。

关键词：V含量；NiTi形状记忆合金；微观组织；马氏体相变；显微硬度